Biochimica et Biophysica Acta 1837 (2014) 246–250

Contents lists available at ScienceDirect

Biochimica et Biophysica Acta

journal homepage: www.elsevier.com/locate/bbabio

Oxidoreduction properties of bound ubiquinone in Complex I from *Escherichia coli*

Marina Verkhovskaya *, Mårten Wikström

Helsinki Bioenergetics Group, Institute of Biotechnology, University of Helsinki, PO Box 65 (Viikinkaari 1), FIN-00014 Helsinki, Finland

ARTICLE INFO

Article history:
Received 19 September 2013
Received in revised form 31 October 2013
Accepted 4 November 2013
Available online 9 November 2013

Keywords:
Complex I
Bound ubiquinone
Redox spectrum
Mid UV-range

ABSTRACT

The exploration of the redox chemistry of bound ubiquinone during catalysis is a prerequisite for the understanding of the mechanism by which Complex I (nicotinamide adenine dinucleotide (NADH):ubiquinone oxidoreductase) transduces redox energy into an electrochemical proton gradient. Studies of redox dependent changes in the spectrum of Complex I from *Escherichia coli* in the mid- and near-ultraviolet (UV) and visible areas were performed to identify the spectral contribution, and to determine the redox properties, of the tightly bound ubiquinone. A very low midpoint redox potential (<−300 mV) was found for the bound ubiquinone, more than 400 mV lower than when dissolved in a phospholipid membrane. This thermodynamic property of bound ubiquinone has important implications for the mechanism by which Complex I catalyzes proton translocation.

1. Introduction

The energy-converting Complex I (NADH:ubiquinone oxidoreductase) operates as an electron input to the respiratory chains of mitochondria and many prokaryotes, and conserves energy by functioning as a redox-linked proton pump. The intraprotein chain of redox centers in Complex I is represented by FMN and 7 FeS clusters, all situated in the hydrophilic domain of the enzyme [1–3]. Redox transitions in these centers can be detected by optical, near-UV and visible range [4–6], ATR-FTIR [7], EPR (e.g. [2,6,8]) and Mössbauer [9] spectroscopy, and have been intensively studied. However, the unique structure of the enzyme where the electron transfer chain and proton translocation sites are well separated spatially [10–12], and functional studies showing lack of a significant energy drop upon electron transfer along the chain (for a review see [13]), make it very likely that this intraprotein chain serves only as a wire to deliver electrons from NADH to the last FeS cluster, N2, which is the neighbor of the ubiquinone binding site. Thus, electron transfer along the chain of FeS centers is hardly coupled to energy conversion, which is expected to occur only upon or after ubiquinone reduction, coupled to conformational changes in the membrane domain. Recently, it was suggested that the unique amphipathic α-helix running parallel to the membrane plane, and connecting three large proton-translocating membrane subunits, would move as a mechanical piston that tilts the α-helices of the proton channels resulting in proton translocation [11,12]. However, the results from several modifications of this α-helix using a molecular biology approach argued against such a mechanical role of this amphipathic helix [14]. Some conformational changes have been detected by electron microscopy [15], FTIR spectroscopy [16,17], and spin labeling [18], but due to the complex protein structure the assignment of these changes remains unclear. In any case, ubiquinone reduction precedes the conformational changes that are coupled to proton translocation.

Several hypotheses of Complex I operation based on ubiquinone transitions are currently under discussion (see [13] for a review). Therefore, detection and monitoring these transitions could be important for revealing the molecular mechanism. So far there is no consensus on whether isolated Complex I contains bound ubiquinone. It was not observed in the resolved structure of Complex I from *Thermus thermophilus* [19], but an equimolar amount has been found in the purified enzymes from *Escherichia coli* [20] and mitochondria [21]. One key question, which is important for understanding the function of Complex I, is whether there are one or two ubiquinone binding sites, for tightly bound and pool-exchangeable ubiquinone. On the one hand, analysis of the Complex I crystal structure showed only one ubiquinone binding site [19], but on the other, the EPR signals of two semiquinone radicals, fast and slow relaxing, were detected in mitochondrial Complex I (e.g. [22,23]). To solve this apparent contradiction the observation of optical spectra of ubiquinone in Complex I would be helpful.

The first attempts to resolve redox spectra of Complex I in the mid- and near-UV range were done with enzymes from *Neurospora crassa* by Schulte at al. [4]. An NADH-dependent peak at 300 nm was detected, which, nevertheless was not assigned to any particular redox group in further studies, and no absorption derived from ubiquinone was reported. We detected redox-dependent absorption changes at 270–280 nm

Abbreviations: SHE, standard hydrogen electrode; E_h, ambient redox potential relative to SHE; E_m, midpoint redox potential relative to SHE; $E_{m,7}$, midpoint redox potential at pH = 7, relative to SHE; LDH, lactate dehydrogenase; GDH, glucose dehydrogenase; HEPES, 4-(2-hydroxyethyl)-1-piperazineethanesulfonic acid; τ, time constant

* Corresponding author. Tel.: +358 9 191 59749; fax: +358 9 191 58003.
E-mail address: Marina.Verkhovskaya@Helsinki.Fi (M. Verkhovskaya).

0005-2728/$ – see front matter © 2013 Elsevier B.V. All rights reserved.
http://dx.doi.org/10.1016/j.bbabio.2013.11.001

characteristic for ubiquinone in samples of purified Complex I from *E. coli*, which we found contains ca. one ubiquinone molecule per FMN, both upon fast reduction by NADH, and in equilibrium spectroelectrochemical redox titrations [20]. These approaches have both advantages and disadvantages. Fast reduction by NADH allows one to conclude that the band derives from the enzyme and not from a contamination. On the other hand, only a low concentration of NADH can be used in order not to overwhelm the enzyme spectrum; therefore Complex I can be reduced only to a low extent. The electrochemical redox titration allows the observation of the Complex I spectrum in the absence of NADH. However, at low (<−300 mV) potentials the used mediators were insufficient to equilibrate the enzyme with the working electrode, and commonly used low-potential mediators, such as methylviologen ($E_m = -430$ mV) and benzylviologen ($E_m = -330$ mV), could not be used due to their strong absorption in the UV range.

Here we report studies of the spectrum of purified Complex I in the mid- and near-UV range using a different technique, which enables us to characterize redox-dependent signals that prove to be due to enzyme-bound ubiquinone.

2. Materials and methods

2.1. Bacterial growth and purification of Complex I

The *E. coli* MWC215 (Sm^R *ndh*::Cm^R) strain was grown in LB medium at 37 °C in a 25 l fermenter and harvested at the late exponential growth phase. The membranes for Complex I purification were prepared by passing the cells through an APV Gaulin homogenizer. Then Complex I was purified by two consecutive chromatography steps using DEAE-Trisacryl M (Bio-Sepra) anion exchanger columns and gel filtration on Superdex 200 prep grade (GE Healthcare), respectively, as described [14].

2.2. Kinetic measurements

Kinetic measurements were carried out at RT using a high-resolution CCD-array spectrometer (HR2000+, Ocean Optics) combined with a DH-2000-BAL light source with filtering technology that produces a smooth spectrum across the entire range (Ocean Optics). The assay buffer comprised 50 mM HEPES–KOH, pH 7.0, 15% glycerol and 0.005% n-dodecyl β-D-maltopyranoside. Complex I was added at a concentration of 1–1.2 μM. Two NADH regenerating systems were used: i) lactate/LDH (lactate 50 mM, LDH 5 μg/ml) and ii) glucose/GDH (glucose 20 mM GDH (from *Pseudomonas* sp., Sigma) 10 μg/ml). In both cases NAD was added to a concentration of 4–5 μM. The samples were prepared anaerobically by purging with argon. Upon kinetic measurements the anaerobiosis was supported by blowing argon through the cuvette. The reaction was initiated by the addition of LDH or GDH, the spectra of cytochrome contamination and added LDH and GDH were subtracted from the spectra of Complex I (the redox changes in these enzymes were not detectable due to their low concentration; Complex I spectra were corrected only for a constant small peak at 280 nm derived from LDH and GDH).

2.3. Data analysis

Data analysis was carried out using the MATLAB software (the Mathworks, Inc.). The decomposition of the kinetic data surfaces was achieved by global fitting run under a MATLAB interface using the Rakowsky algorithm [24].

3. Results and discussion

We used two different NADH-regenerating systems to generate redox spectra of Complex I, viz. lactate/LDH and glucose/GDH. The redox couples lactate/pyruvate ($E_{m,7} = -185$ mV) and glucose/gluconolactone ($E_{m,7} = -470$ mV) [25] are strongly reducing. Therefore, in the absence of pyruvate or gluconolactone, and at a high concentration of lactate or glucose, the operation of LDH and GDH maintains a stable, relatively high NADH/NAD^+ ratio. Since both these nucleotides have absorption bands in the UV range that overlap the Complex I spectrum, a low concentration is required for good resolution. The reduction of Complex I with NADH alone at low concentration was not successful, because then the NADH level dropped fast (and the level of NAD^+ rose) due to enzyme reduction and unspecific electron leakage. The NADH-regenerating systems are therefore advantageous.

The redox potential can be roughly estimated from the NADH/NAD^+ ratio measured optically, because in the absence of added electron acceptors there is very slow unspecific electron flux to some unidentified acceptors. Upon the reduction of Complex I by NADH in the presence of lactate/LDH the calculated E_h is maintained at −270 to −290 mV, under which conditions the enzyme is reduced only partially. A trough in the visible area at 430–460 nm and a small trough at 275–280 nm are observed in the redox (reduced *minus* oxidized) spectrum, together with a broad positive band between 240 and 350 nm and a small peak at 300 nm (Fig. 1). The glucose/GDH system decreases the E_h from −330 to −350 mV. Under these conditions the redox spectrum has a similar shape as before, but now a further reduction of the enzyme can be detected by the absorption decrease in the visible area. In the UV range the trough at 275–280 nm now develops to a considerable extent. The peak at 300 nm hardly changes and is likely to be due to the combined effect of negative absorption at 275–280 nm and the monotonous absorption increase below 350 nm (Fig. 1). The spectrum of Complex I at the higher redox potential, in the presence of lactate/LDH, observed here is similar to those obtained earlier by a partial reduction of Complex I by a low NADH concentration using the stopped-flow technique [20], and to the spectrum of Complex I from *Neurospora crassa* obtained by Shulte et al. [4]. At the higher potentials the trough at 280 nm is very small (Fig. 1), as also observed by Shulte et al. [4], which is why only the peak at 300 nm was considered by these authors, who did not detect any ubiquinone in their preparation of Complex I from *N. crassa* [4]. Our preparation of Complex I from *E. coli* contains 1–1.3 mol Q per 1 mol FMN and the extinction of the observed maximal trough at 270–280 nm roughly corresponds to such a ubiquinone content (Fig. 1; black curve), as also indicated by the redox spectrum of ubiquinone-1 (Fig. 1; red dotted curve). Our data suggests that the deep trough at ~275 nm is due to the bound ubiquinone, very little of which is reduced at the potential of the lactate/LDH system ($E_h = -280$ mV), but which is highly reduced at the potential of the

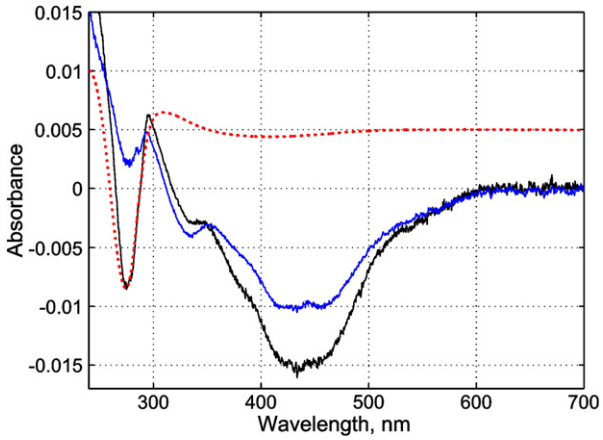

Fig. 1. Redox spectra of Complex I from *E. coli* obtained by NADH regeneration systems, lactate/LDH ($E_h \approx -280$ mV), blue, or glucose/GDH ($E_h < -330$ mV), black. The NAD^+/NADH difference spectra are subtracted from the spectra. Concentration of Complex I is approximately 1 μM. For comparison, the redox spectrum of 1 μM Q1 is shown by the red dotted line shifted on the y-axis by 0.005.

glucose/GDH system (<−330 mV). To test which changes in the visible range (absorption of FeS clusters and FMN) correlate with changes in UV we performed kinetic measurements starting the reaction by GDH addition. Due to the low affinity of GDH for NAD^+ its conversion to NADH is slow, in the seconds range. During this time the NADH/NAD^+ ratio is increased and Complex I is reduced gradually. Since the rate of NADH generation by GDH is much slower than Complex I reduction, the redox sites of the enzyme stay close to equilibrium with the NADH/NAD^+ couple, and the data can be considered as an analog of a redox titration. Although the ambient redox potential cannot be exactly determined, the data gives important semiquantitative redox information.

An example of the obtained set of spectra is shown in Fig. 2A. Global fitting of the kinetic data surface clearly yielded three spectral components (Fig. 2B). The first component (with $\tau < 1$ s), where the NADH concentration is below the measurement limits, shows a reduction of the FeS clusters with the highest redox potential, N1a and N2 [6], a broad trough with minima at 410 and 460 nm, as well as a trough at 330 nm. Also, towards the UV domain the absorption increases monotonously approaching a maximum at 250 nm. The second component ($\tau = 2$–6 s) comprises the spectra of an almost full reduction of NAD^+ (at 340 nm), and also a smaller trough of FeS clusters with lower E_m at ~430 nm. The small trough at 270–280 nm is practically masked by the spectrum of the NAD^+/NADH transition. The control spectrum of the reduction of NAD^+ in the same conditions, but in the absence of Complex I, is shown in Fig. 2B (red curve). This analysis indicates that the clear trough at 270–275 nm develops mainly during the last and slowest phase ($\tau > 100$ s; Fig. 2B), once again suggesting that the reduction of bound ubiquinone occurs only at redox potentials significantly lower than the $E_{m,7}$ of the NADH/NAD^+ couple (−320 mV). This trough is not due to a reduction of FMN because it is not accompanied by an absorption decrease in the 440–460 nm region [20].

Another approach, in which the difference spectra were taken at specific time intervals, provides more detailed data. The absorption at 340 nm, which derives mainly from the reduction of NAD^+ to NADH, was plotted against time and the resulting sigmoid curve was divided into five time intervals, as shown in Fig. 3A. Fig. 3B shows the difference spectra between the end and the beginning of each interval, after subtracting the spectrum due to NAD^+ reduction in intervals III and IV. The NADH concentration is below the measurement limits during

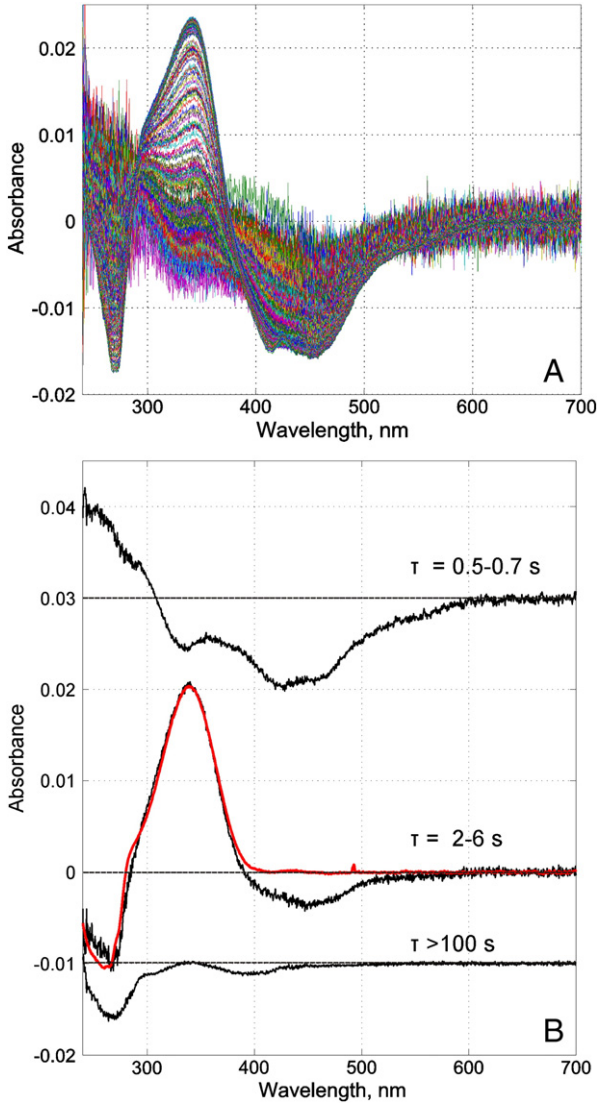

Fig. 2. Kinetics of anaerobic Complex I reduction by NADH regenerating GDH/glucose system. A. Set of spectra taken after the reaction was initiated by GDH addition and followed for 6 min. B. Spectral components obtained by global fitting of the experimental data. The first component ($\tau < 1$ s) represents the reduction of FeS clusters with the highest E_m, N1a and N2, and a broad peak in the UV area derived from an unidentified chromophore. The second component shows NADH reduction by GDH and further reduction of Complex I. The slowest ($\tau > 100$ s) component is represented by the trough at 270–275 nm. Dashed lines indicate a zero level of absorption in each spectrum.

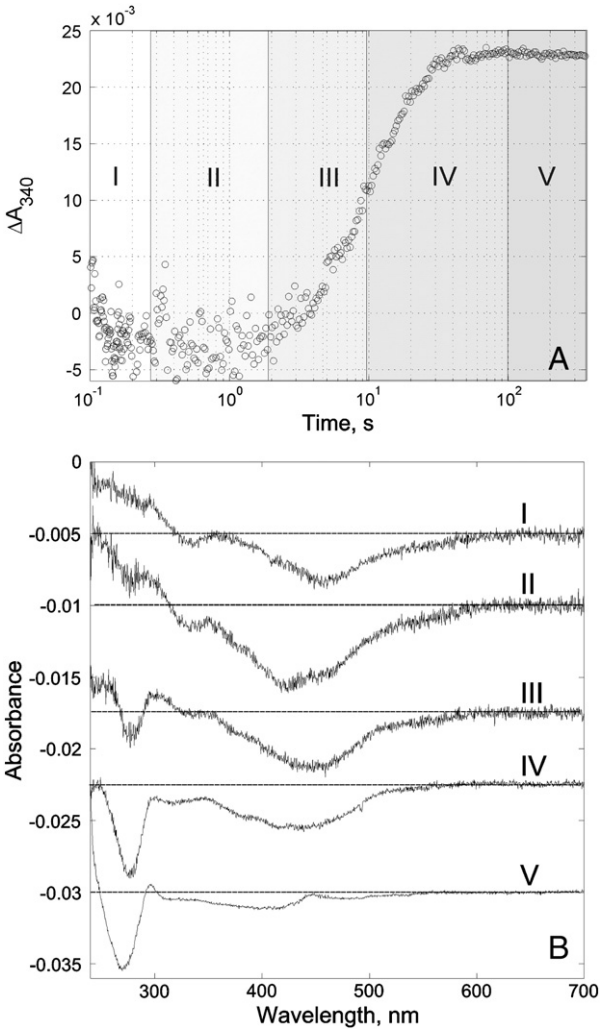

Fig. 3. Differential redox spectra of Complex I taken at particular time intervals upon its reduction. A. Kinetics of NADH increase after GDH addition divided into five time intervals: I, 0.6 s; II, 0.6–2 s; III, 2–10 s; IV, 10–100 s; V, 100 s–6 min. B. Differential spectra of Complex I reflecting the events, which occur in the enzyme in particular time and, consequently, E_h intervals. The NAD^+/NADH transition spectra are subtracted from the spectra of phases III and IV. Dashed lines indicate a zero level of absorption in each spectrum.

the first two intervals, and the E_h is relatively high, well above −290 mV at which potential the NAD^+ would be 10% reduced. Broad minima develop at 420–460 and 330 nm, probably mostly due to a reduction of the binuclear FeS center N1a and the tetranuclear center N2, although other FeS centers that have more negative midpoint potentials could contribute to a lesser extent [6]. In the third interval E_h decreased to approximately −320 mV, close to the potential at which NAD^+ is 50% reduced (see Fig. 3A), and a clear negative peak develops at ~275 nm together with a broad trough at 450 nm. In the fourth interval NAD^+ became more than 90% reduced, so that the E_h dropped to <−350 mV. The optical pattern is similar to that of interval III except that now the trough at ~275 nm is larger and the trough at 450 nm is slightly smaller. The redox potential dropped further in the fifth interval, because additional reduction is seen by the deep trough at 271–275 nm, but now the redox state of NAD^+ can no longer be used to calibrate the E_h. The $E_{m,7.5}$ of FMN is −350 mV in Complex I from *E. coli* [6], and thus it is expected to be partially reduced in the intervals III–IV, which is consistent with the trough at 275 nm accompanied by the broad negative absorption at 440–445 nm [20], although part of the latter is due to low-potential FeS clusters. The fifth interval shows a considerable trough at 271–275 nm, slightly blue-shifted in comparison with previous phases, which is not accompanied by any significant absorption decrease at 440–450 nm typical of FMN reduction [20]. It is noteworthy that adding the strong reductant dithionite after the fifth interval still caused further reduction that was observed as troughs at 271–275 nm and at 440–450 nm, where the amplitude of both bands was increased by 30–40% relative to the combined troughs of intervals I–V (not shown).

Similar results were obtained upon the reduction of Complex I in the presence of the specific inhibitor, rolliniastatin (not shown). The lack of a rolliniastatin effect could be explained irrespective of the number of ubiquinone binding sites. In case of only one site, the rolliniastatin could bind in a way that prevents the movement of the bound quinone, but not its reduction. In case of two sites, the rolliniastatin could bind to the weak binding site for pool-exchangeable ubiquinone, and would therefore not affect the reduction of tightly bound ubiquinone.

The differential spectra in the same conditions, but in the presence of added DQ are shown in Fig. 4. The enzyme (1 μM) was incubated with 4.6 μM DQ for 10 min before the reaction was started. The kinetics was divided into the same time intervals as previously. In the first two intervals at low NADH concentration, only a partial reduction of FeS clusters was observed together with a small trough in the ubiquinone band. Otherwise, the absorbance changes were the same as in the absence of DQ. In the third interval, before any significant reduction of NAD^+, a large trough at 277 developed, clearly due to the reduction of DQ; NADH was consumed and its concentration stayed low which explains the low reduction level of FeS centers. During this phase ~3.0 μM of DQ was reduced. In interval IV almost all of the NAD^+ was reduced, indicating that electron flux to DQ had stopped. However, the increase of the trough at 277 nm continued, either due to a very slow reduction of the rest of the added DQ or to some fraction of DQ that was initially distributed to Complex I-free detergent micelles, and exchange between the micelles is slow [26], or a reduction of ubiquinone bound to the enzyme, or both. In the last interval V again only the trough at 275 nm was observed, also slightly blue-shifted, with the same amplitude as in the absence of added quinone, and unaccompanied by a trough at 440–450 nm. The spectrum of interval V again suggests a reduction of bound ubiquinone at a low redox potential.

It should be noted that the spectra during the first two seconds after GDH addition (intervals I and II) are almost identical to those in the absence of DQ, which means that DQ ($E_m \approx 110$ mV) reduction starts only in the interval III although the redox potential is low enough as indicated by the observed reduction of some FeS clusters (N1a $E_m = -235$ mV, N2 $E_m^1 = -200$ mV, $E_m^2 = -300$ mV [6]). This delay could reflect a lag phase in the enzyme activity observed earlier [27], or it could be due to the system being in a steady state of flux in which near redox equilibrium is established among the fast electron

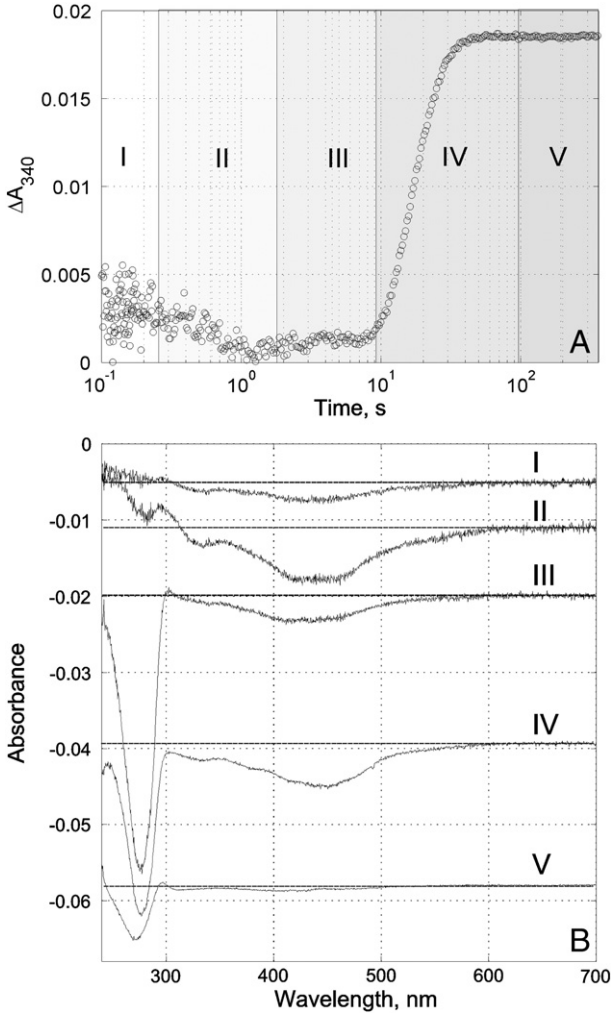

Fig. 4. Differential redox spectra of Complex I taken at particular time intervals upon its reduction in the presence of DQ. DQ was added to a concentration of 4.5 μM. A. Kinetics of NADH increase after GDH addition divided into five time intervals: I, 0.6 s; II, 0.6–2 s; III, 2–10 s; IV, 10–100 s; V, 100 s–6 min. B. Differential spectra of Complex I reflecting the events, which occur in the enzyme at particular time and, consequently, E_h intervals. NAD^+/NADH transition spectra are subtracted from the spectra of phases III and IV. Dashed lines indicate a zero level of absorption in each spectrum.

transfer reactions between the NAD^+/NADH couple and the array of FeS centers, but not including the acceptor DQ [13,28].

The observed redox changes in the Complex I spectrum in the mid- and near-UV regions are not dependent on the enzyme activity. The only factor they are dependent on is the ambient redox potential established by the NADH/NAD^+ pair. The very broad positive absorption below 300 nm develops at relatively high E_h (>−300 mV), and may reflect a structural rearrangement in the enzyme due to the reduction of the high potential FeS clusters.

Two components besides ubiquinone could contribute to the trough at 271–280 nm, FMN and aromatic amino acid residues. The absorption changes due to structural changes of aromatic residues upon reduction could contribute to the band, but only to a small extent due to the low molar absorptivities involved. The band at 275–280 nm can only partially be ascribed to FMN, viz. in intervals III–IV (Fig. 3). In interval V this band can be ascribed solely to bound ubiquinone, because it is not accompanied with changes in the visible area at 450 nm which are characteristic for flavin. The total extinction of the band at 270–280 nm roughly corresponds to 1 mol of ubiquinone per 1 mol of Complex I, and is therefore too small to accommodate both ubiquinone and flavin. This conundrum is explained by the finding that dithionite increases the amplitude of the 270–280 nm band to an extent that it

then could be compatible with both FMN and bound ubiquinone. However, the exact size and shape of this band is uncertain due to the absorption of products of dithionite oxidation in the UV. At the same time dithionite induces a significant trough at 440–460 nm, so most of the dithionite-induced change is likely to be due to a reduction of FMN. The reason for the requirement of dithionite to fully reduce FMN may have the same origins as recently described [29]: for kinetic reasons FMN is reduced only to a small extent by NADH, even at low potentials.

This work confirms our previous observations of the presence of a bound, redox-active ubiquinone in Complex I from *E. coli* [20]. Its apparent midpoint redox potential is substantially lower than the previously estimated upper limit, and is at least as low as −300 mV. The reduced species is ubiquinol in the current work, because ubisemiquinone has absorption near 320 nm with a molar absorptivity high enough to have been identified here if present to a significant degree [30,31]. This is also confirmed by our previous observation of the lack of the radical signal of ubisemiquinone in the EPR spectra of Complex I from *E. coli* reduced by NADH [6,28,32]. On the other hand, we cannot distinguish whether, or to what extent, the reduced bound ubiquinone is protonated in our titrations. The lack of or incomplete protonation of the bound ubiquinone is the most likely reason for the lowered redox potential. The other possible reason is much tighter binding of the oxidized than of the reduced form of this cofactor. These two possibilities are not mutually exclusive, but there is no example in the literature of the very much stronger binding of Q than of QH_2 that would be required to explain the >400 mV shift in E_m. Since the E_m of the bound ubiquinone is lower than −300 mV, its reduction by NADH cannot provide the driving force for proton translocation. Hence, it is the free energy change associated with reactions beyond the reduction of the bound ubiquinone that drives proton pumping.

Acknowledgements

This work was supported by grants from Biocentrum Helsinki, the Sigrid Juselius Foundation, and the Academy of Finland. We thank Eija Haasanen for purification of Complex I.

References

[1] T. Ohnishi, V.D. Sled, T. Yano, T. Yagi, D.S. Burbaev, A.D. Vinogradov, Structure–function studies of iron–sulfur clusters and semiquinones in the NADH-Q oxidoreductase segment of the respiratory chain, Biochim. Biophys. Acta 1365 (1998) 301–308.
[2] T. Ohnishi, Iron–sulfur clusters/semiquinones in Complex I, Biochim. Biophys. Acta 1364 (1998) 186–206.
[3] P. Hinchliffe, L.A. Sazanov, Organization of iron–sulfur clusters in respiratory Complex I, Science 309 (2005) 771–774.
[4] U. Schulte, A. Abelmann, N. Amling, B. Brors, T. Friedrich, L. Kintscher, T. Rasmussen, H. Weiss, Search for novel redox groups in mitochondrial NADH:ubiquinone oxidoreductase (Complex I) by diode array UV/VIS spectroscopy, Biofactors 8 (1998) 177–186.
[5] T. Rasmussen, D. Scheide, B. Brors, L. Kintscher, H. Weiss, T. Friedrich, Identification of two tetranuclear FeS clusters on the ferredoxin-type subunit of NADH:ubiquinone oxidoreductase (Complex I), Biochemistry 40 (2001) 6124–6131.
[6] L. Euro, D.A. Bloch, M. Wikström, M.I. Verkhovsky, M. Verkhovskaya, Electrostatic interactions between FeS clusters in NADH:ubiquinone oxidoreductase (Complex I) from *Escherichia coli*, Biochemistry 47 (2008) 3185–3193.
[7] D. Marshall, N. Fisher, L. Grigic, V. Zickermann, U. Brandt, R.J. Shannon, J. Hirst, R. Lawrence, P.R. Rich, ATR-FTIR redox difference spectroscopy of *Yarrowia lipolytica* and bovine Complex I, Biochemistry 45 (2006) 5458–5467.
[8] V. Zickermann, K. Zwicker, M.A. Tocilescu, S. Kerscher, U. Brandt, Characterization of a subcomplex of mitochondrial NADH:ubiquinone oxidoreductase (Complex I) lacking the flavoprotein part of the N-module, Biochim. Biophys. Acta 1767 (2007) 393–400.
[9] H.R. Bridges, E. Bill, J. Hirst, Mössbauer spectroscopy on respiratory Complex I: the iron–sulfur cluster ensemble in the NADH-reduced enzyme is partially oxidized, Biochemistry 51 (2012) 149–158.
[10] J.M. Berrisford, L.A. Sazanov, Structural basis for the mechanism of respiratory Complex I, J. Biol. Chem. 284 (2009) 29773–29783.
[11] R.G. Efremov, L.A. Sazanov, Structure of the membrane domain of respiratory Complex I, Nature 476 (2011) 414–420.
[12] R.G. Efremov, L.A. Sazanov, The coupling mechanism of respiratory Complex I — a structural and evolutionary perspective, Biochim. Biophys. Acta 1817 (2012) 1785–1795.
[13] M. Verkhovskaya, D.A. Bloch, Energy-converting respiratory Complex I: on the way to the molecular mechanism of the proton pump, Int. J. Biochem. Cell Biol. 45 (2013) 491–511.
[14] G. Belevich, J. Knuuti, M.I. Verkhovsky, M. Wikström, M. Verkhovskaya, Probing the mechanistic role of the long alpha-helix in subunit L of respiratory Complex I from *Escherichia coli* by site-directed mutagenesis, Mol. Microbiol. 82 (2011) 1086–1095.
[15] A.A. Mamedova, P.J. Holt, J. Carroll, L.A. Sazanov, Substrate-induced conformational change in bacterial Complex I, J. Biol. Chem. 279 (2004) 23830–23836.
[16] P. Hellwig, S. Stolpe, T. Friedrich, Fourier transform infrared spectroscopic study on the conformational reorganization in *Escherichia coli* Complex I due to redox-driven proton translocation, Biopolymers 74 (2004) 69–72.
[17] T. Friedrich, P. Hellwig, Redox-induced conformational changes within the *Escherichia coli* NADH ubiquinone oxidoreductase (Complex I): an analysis by mutagenesis and FT-IR spectroscopy, Biochim. Biophys. Acta 1797 (2010) 659–663.
[18] T. Pohl, D. Schneider, R. Hielscher, S. Stolpe, K. Dorner, M. Kohlstadt, B. Bottcher, P. Hellwig, T. Friedrich, Nucleotide-induced conformational changes in the *Escherichia coli* NADH:ubiquinone oxidoreductase (Complex I), Biochem. Soc. Trans. 36 (2008) 971–975.
[19] R. Baradaran, J.M. Berrisford, G.S. Minhas, L.A. Sazanov, Crystal structure of the entire respiratory Complex I, Nature 494 (2013) 443–448.
[20] M. Verkhovsky, D.A. Bloch, M. Verkhovskaya, Tightly-bound ubiquinone in the *Escherichia coli* respiratory Complex I, Biochim. Biophys. Acta 1817 (2012) 1550–1556.
[21] K. Shinzawa-Itoh, J. Seiyama, H. Terada, R. Nakatsubo, K. Naoki, Y. Nakashima, S. Yoshikawa, Bovine heart NADH-ubiquinone oxidoreductase contains one molecule of ubiquinone with ten isoprene units as one of the cofactors, Biochemistry 49 (2010) 487–492.
[22] S. Magnitsky, L. Toulokhonova, T. Yano, V.D. Sled, C. Hägerhäll, V.G. Grivennikova, D.S. Burbaev, A.D. Vinogradov, T. Ohnishi, EPR characterization of ubisemiquinones and iron–sulfur cluster N2, central components of the energy coupling in the NADH-ubiquinone oxidoreductase (Complex I) in situ, J. Bioenerg. Biomembr. 34 (2002) 193–208.
[23] S.T. Ohnishi, J.C. Salerno, T. Ohnishi, Possible roles of two quinone molecules in direct and indirect proton pumps of bovine heart NADH-quinone oxidoreductase (Complex I), Biochim. Biophys. Acta 1797 (2010) 1891–1893.
[24] D.A. Bloch, A. Jasaitis, M.I. Verkhovsky, Elevated proton leak of the intermediate OH in cytochrome c oxidase, Biophys. J. 96 (2009) 4733–4742.
[25] H.K. Chenault, E.S. Simon, G.M. Whitesides, Cofactor regeneration for enzyme-catalysed synthesis, Biotechnol. Genet. Eng. Rev. 6 (1988) 221–270.
[26] V.P. Shinkarev, C.A. Wraight, The interaction of quinone and detergent with reaction centers of purple bacteria. I. Slow quinone exchange between reaction center micelles and pure detergent micelles, Biophys. J. 72 (1997) 2304–2319.
[27] M. Verkhovskaya, J. Knuuti, M. Wikström, Role of Ca^{2+} in structure and function of Complex I from *Escherichia coli*, Biochim. Biophys. Acta 1807 (2011) 36–41.
[28] M.L. Verkhovskaya, N. Belevich, L. Euro, M. Wikström, M.I. Verkhovsky, Real-time electron transfer in respiratory Complex I, Proc. Natl. Acad. Sci. U. S. A. 105 (2008) 3763–3767.
[29] J. Knuuti, G. Belevich, V. Sharma, D.A. Bloch, M. Verkhovskaya, A single amino acid residue controls ROS production in the respiratory Complex I from *Escherichia coli*, Mol. Microbiol. (2013)(in press).
[30] M. Bauscher, E. Nabedryk, K. Bagley, J. Breton, W. Mantele, Investigation of Models for Photosynthetic Electron-Acceptors — Infrared Spectroelectrochemistry of Ubiquinone and Its Anions, FEBS Lett. 261 (1990) 191–195.
[31] E.J. Land, M. Simic, A.J. Swallow, Optical Absorption Spectrum of Half-Reduced Ubiquinone, Biochim. Biophys. Acta 226 (1971) 239.
[32] L. Sinegina, M. Wikström, M.I. Verkhovsky, M.L. Verkhovskaya, Activation of isolated NADH:ubiquinone reductase I (Complex I) from *Escherichia coli* by detergent and phospholipids. Recovery of ubiquinone reductase activity and changes in EPR signals of iron–sulfur clusters, Biochemistry 44 (2005) 8500–8506.